Journal of Superconductivity and Novel Magnetism (2018) 31:3075–3078
https://doi.org/10.1007/s10948-018-4807-4

LETTER

High-Field Magneto-Conductivity Analysis of Bi_2Se_3 Single Crystal

Rabia Sultana[1,2] · Ganesh Gurjar[3] · S. Patnaik[3] · V. P. S. Awana[1,2]

Received: 2 July 2018 / Accepted: 7 July 2018 / Published online: 13 July 2018

Abstract
We report the high-field (up to 14 Tesla) magneto-conductivity analysis of Bi_2Se_3 topological insulator grown via the self-flux method. The detailed experimental investigations including crystal growth as well as the electrical, thermal, and spectroscopic characterizations of the resultant Bi_2Se_3 single crystal are already reported by some of us. The current letter deals with high-field magneto-conductivity analysis in terms of Hikami Larkin Nagaoka (HLN) model, which revealed that the electronic conduction is dominated by both surface state-driven weak anti-localization (WAL), as well as the bulk weak localization (WL) states. Further, by applying the HLN equation, we have extracted the fitting parameters, i.e., phase coherence length (l_φ) and the pre-factor (α). Here, the magneto-conductivity data is fitted up to ± 5 Tesla, but in order to extract reliable fitting parameters, the same is fitted at much lower magnetic fields, i.e., up to ± 1 Tesla. The value of the HLN coefficient (α), extracted from the HLN equation exhibited values close to − 1.0, indicating both WAL and WL contributions. On the other hand, the extracted l_φ is seen to decrease from 11.125 to 5.576 nm as the temperature is increased from 5 to 200 K, respectively. Summarily, the short letter discusses primarily the temperature-dependent magneto-conductivity analysis of pristine Bi_2Se_3 single crystal by the HLN model.

Keywords Topological insulator · Crystal growth · Magneto-conductivity

1 Introduction

Three-dimensional (3D) layered materials popularly known as the topological insulators (TIs) are one of the novel materials discovered recently [1–3]. Bi_2Te_3, Bi_2Se_3, and Sb_2Te_3 are among the most extensively studied 3D TI materials due to their single surface Dirac cone along with a relatively large bulk energy gap [1–4]. These layered materials represent a new phase of quantum matter exhibiting simultaneously bulk band gap in the interior and the gapless electronic surface states protected by time reversal symmetry (TRS) [1–6]. Historically, these TIs were known to be good thermoelectric materials, but owing to their exotic surface states and unusual magnetic properties, these now hold great promises for novel applications such as spintronics and quantum computers owing to fascinating quantum effects and topological order [1–6]. The existence of the topological surface states has been experimentally confirmed by the angle-resolved photoemission spectroscopy (ARPES) and scanning tunneling microscopy (STM) measurements [4–6]. Indeed, various quantum transport phenomenon viz. weak anti-localization (WAL), quantum conductance fluctuation, Aharonov-Bohm (AB) oscillations, and high-field linear magneto-resistance (MR) associated with the topological surface states are already attracting huge attention from the scientific community [7–14]. Among these quantum transport phenomena of TIs, the WAL effect arising from the π-Berry phase of the topological surface states act as one of the main driving force behind the unusual MR as well various other intriguing transport feature of TIs [9–14].

However, the electronic transport measurements still remains a challenge, because the surface state-driven WAL is often dominated by the weak localization (WL) bulk contribution to the conduction process. This precisely occurs due to the opening of a surface state gap from say intrinsic defects or unintentional doping giving rise

✉ V. P. S. Awana
awana@nplindia.org
http://awanavps.webs.com

1 CSIR-National Physical Laboratory, Dr. K. S. Krishnan Road, New Delhi, 110012, India

2 Academy of Scientific and Innovative Research (AcSIR)-NPL, New Delhi, 110012, India

3 School of Physical Sciences, Jawaharlal Nehru University, New Delhi, 110067, India

to the WL effect [9–13]. Both WAL and WL are the quantum interference effects, which respectively lead to the enhancement and suppression of the conductivity at lower temperatures. However, in the TI system, the quantum interference effect can be easily destroyed by the application of small magnetic field. WAL appears with the negative magneto-conductivity with a sharp dip (cusp) in lower applied fields, which is well in a system with strong spin-orbit coupling (SOC). On the other hand, WL is seen as cusp-like positive magneto-conductivity at lower applied field and temperatures [9–13].

Experimentally, the analysis of WAL effect in 3D TIs is done by fitting the magneto-conductivity data using the well-known Hikami Larkin Nagaoka (HLN) equation [15]. In the present work, we discuss and analyze our reported high-field linear non-saturating MR behavior of pristine Bi_2Se_3 single crystal [16], in terms of the HLN equation and do conclude that in TIs often both conducting surface-driven WAL and insulating bulk-dominated WL do contribute to the overall conductivity, a result very similar to that as reported by us recently for Bi_2Te_3 [13]. This is further consistent with our recent observations related to unexplored photoluminescence of Bi_2Te_3, showing that TIs do exhibit electronic transitions from bulk insulating interior to conducting surface states [17].

2 Experimental Details

Conventional self-flux method was used to synthesize quality bulk single crystals of Bi_2Se_3. The experimental technique including the crystal growth and the heat treatment diagram along with the structural, micro-structural, spectroscopic, and thermal properties are described in detail in our own past work [16]. As the TIs exhibit a layered structure, the mechanical cleaving was easily performed and the easily cleaved thin flakes of Bi_2Se_3 single crystal revealed a silvery shining mirror-like flat surface. The magneto-transport measurements were carried out on one cleaved flake using 14 Tesla down to 2 K, Quantum Design Physical Property Measurement System (PPMS), Model 6000 equipped with standard four-probe technique. Silver paste was employed for making electrical transport contacts on freshly cleaved shining surface of the crystal.

3 Results and Discussion

Figure 1 displays the single crystal X-ray diffraction (XRD) pattern of as-synthesized Bi_2Se_3 recorded using the Rigaku-Miniflex II having Cu-K_α radiation ($\lambda = 1.5418$ Å). The X-ray analysis was carried out on the cleaved silvery surface of the Bi_2Se_3 single crystal. The XRD diffraction

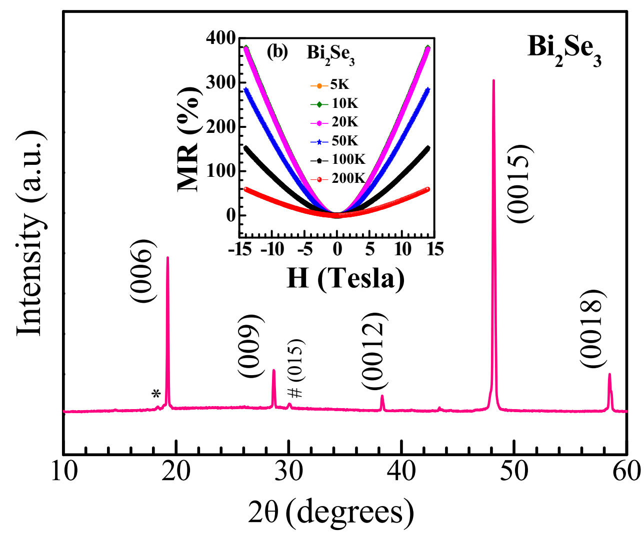

Fig. 1 X-ray diffraction pattern of as-synthesized Bi_2Se_3 single crystal. Inset shows the percentage change of magneto-resistance at different temperatures for Bi_2Se_3 single crystal

spectra revealed highly indexed peaks with (00l) reflections, indicating the crystalline nature of the synthesized Bi_2Se_3 crystal. Also to be noted that tiny peaks around 18.5° and 30° do appear, the later one is due to the misaligned [015] plane of Bi_2Se_3, and the former is not identified. The said peaks are marked in Fig. 1 as well. Further, the powder XRD patterns confirmed the rhombohedral crystal structure of the as-synthesized Bi_2Se_3 single crystal; more details are given in ref. [16].

The inset of Fig. 1 shows the typical percentage change of MR of as-grown Bi_2Se_3 single crystal as a function of perpendicularly applied magnetic fields at different temperatures. Here, the MR is calculated using the equation MR (%) $= ((\rho(H) - \rho(0)) / \rho(0)) \times 100$, where $\rho(0)$ and $\rho(H)$ represent the resistivity values under zero and non-zero applied magnetic fields (H), respectively. Apparently, it can be seen that all the MR curves exhibit positive MR values. A linear, non-saturating MR behavior reaching up to a value of about 380% is observed under 14 Tesla and is maintained nearly at the same temperature below 20 K. At 50, 100, and 200 K, the MR reaches a value of about 280, 150, and 60%, respectively, under 14 Tesla applied magnetic field. Also, the shape of the MR curve tends to broaden as the temperature is increased from 5 to 200 K. The quantitative MR (%) values at different temperatures under 14 Tesla applied magnetic field of as-grown Bi_2Se_3 single crystal are listed in Table 1.

Now, to understand the MR behavior shown in the inset of Fig. 1, we employed the HLN equation, which is the main output of the present letter. As discussed, the WAL effect arises from the topological surface states and appears as a negative magneto-conductivity cusp (sharp dip) at

Table 1 MR (%) values at different temperatures under 14 Tesla applied magnetic field as well as HLN fit values of pre-factor (α) and phase coherence length (l_φ) for Bi_2Se_3 crystal

Temperature (K)	α	l_φ (nm)	MR (%) at 14 Tesla
5	−0.9897	11.125	∼ 380
10	−1.040	10.895	∼ 380
20	−1.045	10.667	∼ 380
50	−1.012	9.496	∼ 280
100	−0.999	7.805	∼ 150
200	−0.996	5.576	∼ 60

lower fields. However, with increase in temperature and magnetic field, the sharp cusp-type behavior gradually gets suppressed. This suppression of WAL behavior occurs due to the breaking of TRS induced by magnetic field. In order to analyze the quantum corrections to the conductivity of pristine Bi_2Se_3 single crystal experimentally, the magneto-conductivity curves are fitted using the standard HLN equation [15]

$$\Delta\sigma(H) = \sigma(H) - \sigma(0) = -\frac{\propto e^2}{\pi h}\left(\ln(\frac{B_\varphi}{H}) - \Psi\left(\frac{1}{2} + \frac{B_\varphi}{H}\right)\right)$$

where $\Delta\sigma(H)$ represents the change of magneto-conductivity, Ψ is the digamma function, e is the electronic charge, h is the Planck's constant, $B_\varphi = \frac{h}{8e\pi H l_\varphi}$ is the characteristic magnetic field, and H is the applied magnetic field. Here, l_φ and α are the two fitting parameters signifying phase coherence length and pre-factor, respectively. The pre-factor, α is a coefficient indicating the type of localization (WL, WAL, or both WL and WAL) and exhibits values depending upon the type of spin-orbit interaction (SOI) and magnetic scattering [15]. Accordingly, $\alpha = 0$ when the magnetic scattering is strong, $\alpha = 1$ when the SOI and magnetic scattering is weak or absent, and $\alpha = -1/2$ when SOI is strong and there is no magnetic scattering [15].

Figure 2 depicts the standard HLN fitting of magneto-conductivity curves for Bi_2Se_3 single crystal carried out at various temperatures under an applied magnetic field of ± 5 Tesla. As expected, a negative change in conductance is observed (Figs. 2 and 3). The symbols in Figs. 2 and 3 represent the experimentally observed data, whereas the solid lines correspond to the HLN fitting curves. At lower temperatures (5, 10, and 20 K), the magneto-conductivity curves are observed to overlap on each other whereas, distinct magneto-conductivity curves are seen at temperatures above 20 K. Figure 2 clearly shows that as the temperature increases from 5 to 200 K, the magneto-conductivity curves tend to exhibit less negative values. In consequence, all the magneto-conductivity curves follow HLN behavior.

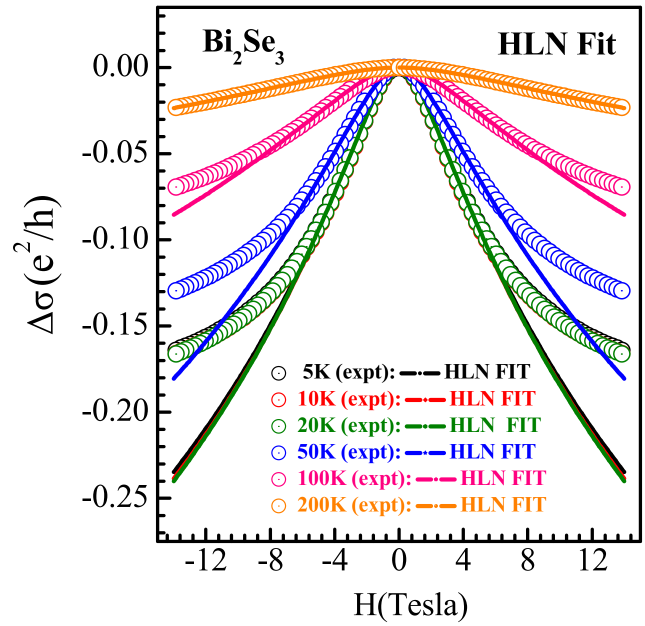

Fig. 2 WAL-related magneto-conductivity for Bi_2Se_3 single crystal at different temperatures (5, 10, 20, 50, 100, and 200 K), fitted using the HLN equation up to ± 5 Tesla

In order to extract reliable fitting parameters (α and l_φ) and to study the HLN equation more specifically, the magneto-conductivity curves at different temperatures are HLN fitted at much lower magnetic fields, i.e., up to ± 1 Tesla as depicted in Fig. 3. The magneto-conductivity curves fits the standard HLN equation quite well and yields

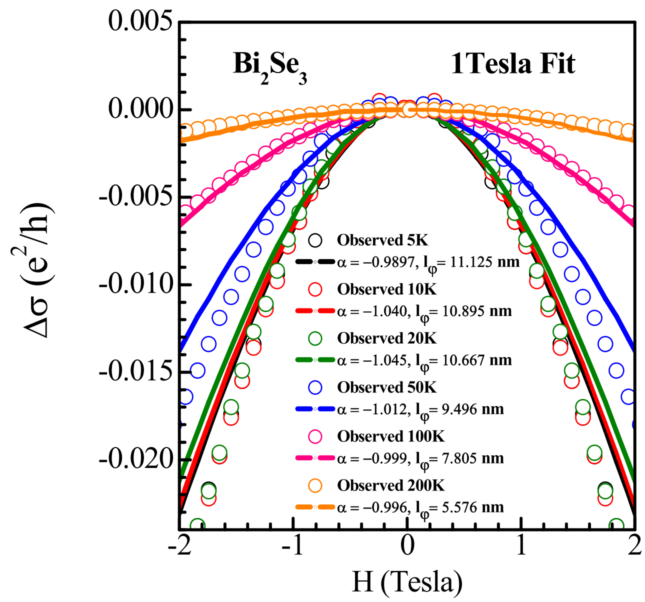

Fig. 3 Magneto-conductivity curves for Bi_2Se_3 single crystal at different temperatures (5, 10, 20, 50, 100, and 200 K), fitted using the HLN equation up to ± 1 Tesla

reasonable values of the fitting parameters (α and l_φ). The fitting parameters (α and l_φ) are provided in a tabular form (Table 1) as well as in Fig. 3 itself. Ideally, the HLN coefficient (α), should be − 1/2 for each transport channel that carries a π-Berry phase or exhibits strong SOI; whereas, for multiple carrier channels (surface and bulk states), the value should add up to a bigger negative value viz. − 1 and − 1.5. Usually, the experimentally fitted value of α covers a wide range from − 0.4 to − 1.1, suggesting that the observed WAL effect arises from single surface state, two surface states, or intermixing between the WAL of the surface states and WL of the bulk states. Accordingly, it becomes difficult to differentiate the conduction taking place from bulk and surface states clearly. Additionally, the fitting parameter (α and l_φ) values depends from material to material viz., bulk single crystals, thin films, nanowires, and thin flakes [9–13].

In our case, the pre-factor, α measuring the strength of WAL is observed to exhibit values close to around − 1, suggesting that both surface (WAL) and bulk states (WL) contribute to the conduction mechanism. Accordingly, the extracted value of α is close to the predicted theoretical value of − 1 for all temperatures (5, 10, 20, 50, 100, and 200 K). Indeed, one can see from Table 1, that the obtained value of α remains nearly unchanged as a function of temperature. However, l_φ is observed to decrease from 11.125 to 5.576 nm at 5 and 200 K, respectively. This decrease in phase coherence length as a function of temperature is expected since the probability of inelastic scattering due to electron-electron interaction increases with temperature. Recently, in the case of Bi_2Te_3 bulk single crystal as well, we found good fitting of magneto-conductivity data to HLN equation with pre-factor (α) close to − 0.9 and l_φ decreasing from 98 to 40 nm with increase in temperature from 2.5 to 50 K [13]. Further, this is consistent with our recent results related to unexplored photoluminescence from bulk and mechanically exfoliated few layers of Bi_2Te_3, exhibiting electronic transition from bulk-insulating to surface-conducting states [17]. The HLN analysis of high-field magneto-conductivity data of both Bi_2Te_3 [13] and presently studied Bi_2Se_3 show the contributions from both WL (bulk-insulating) and WAL (surface-conducting) states to overall conduction of these composite systems.

Summarily, it is seen that the magneto-conductivity of the single crystalline Bi_2Se_3 topological insulator follows the standard HLN model being dominated by both surface- and bulk state-driven WAL and WL processes.

Acknowledgements The authors from CSIR-NPL would like to thank their Director NPL, India, for his keen interest in the present work. Rabia Sultana and Ganesh Gurjar thank CSIR, India for research fellowship. Rabia Sultana thanks AcSIR-NPL for Ph.D. registration.

References

1. Hasan, M.Z., Kane, C.L.: Rev. Mod. Phys. **82**, 3045 (2010)
2. Moore, J.E.: Nature **464**, 194 (2010)
3. Ando, Y.: J. Phys. Soc. Jpn. **82**, 102001 (2013)
4. Zhang, H., Liu, C.-X., Qi, X.-L., Dai, X., Fang, Z., Zhang, S.-C.: Nat. Phys. **5**, 438 (2009)
5. Xia, Y., Qian, D., Hsieh, D., Wray, L., Pal, A., Lin, H., Bansil, A., Grauer, D., Hor, Y.S., Cava, R.J., Hasan, M.Z.: Nat. Phys. **5**, 398 (2009)
6. Zhang, T., Cheng, P., Chen, X., Jia, J.-F., Ma, X., He, K., Wang, L., Zhang, H., Dai, X., Fang, Z., Xie, X., Xue, Q.-K.: Phys. Rev. Lett. **103**, 266803 (2009)
7. Checkelsky, J.G., Hor, Y.S., Liu, M.-H., Qu, D.-X., Cava, R.J., Ong, N.P.: Phys. Rev. Lett. **103**, 246601 (2009)
8. Peng, H., Lai, K., Kong, D., Meister, S., Chen, Y., Qi, X.-L., Zhang, S.-C., Shen, Z.-X., Cui, Y.: Nat. Mater. **9**, 225 (2010)
9. Chen, J., Qin, H.J., Yang, F., Liu, J., Guan, T., Qu, F.M., Zhang, G.H., Shi, J.R., Xie, X.C., Yang, C.L., Wu, K.H., Li, Y.Q., Lu, L.: Phys. Rev. Lett. **105**, 176602 (2010)
10. Lu, H.-Z., Shen, S.-Q.: Phy. Rev. B **84**, 125138 (2011)
11. Cha, J.J., Kong, D., Hong, S.-S., Analytis, J.G., Lai, K., Cui, Y.: Nano Lett. **12**, 1107 (2012)
12. Chiatti, O., Riha, C., Lawrenz, D., Busch, M., Dusari, S., Barriga, J.S., Mogilatenko, A., Yashina, L.V., Valencia, S., Unal, A.A., Rader, O., Fischer, S.F.: Sci. Rep. **6**, 27483 (2016)
13. Sultana, R., Gurjar, G., Neha, P., Patnaik, S., Awana, V.P.S.: J. Supercond. Nov. Magn. https://doi.org/10.1007/s10948-018-4762-0
14. He, H., Li, B., Liu, H., Guo, X., Wang, Z., Xie, M., Wang, J.: Appl. Phys. Lett. **100**, 032105 (2012)
15. Hikami, S., Larkin, A.I., Nagaoka, Y.: Prog. Theor. Phys. **63**, 707 (1980)
16. Sultana, R., Awana, G., Pal, B., Maheshwari, P.K., Mishra, M., Gupta, G., Gupta, A., Thirupathaiah, S., Awana, V.P.S.: J. Supercond. Nov. Magn. **30**, 2031 (2017)
17. Gupta, B.K., Sultana, R., Singh, S., Singh, V., Awana, G., Gupta, A., Singh, B., Srivasatava, A.K., Srivastava, O.N., Auluck, S., Awana, V.P.S.: Sci. Rep. **8**, 2905 (2018)